

Absence of Superconductivity in LiCu_2P_2

Fei Han,[†] Xiyu Zhu,[†] Gang Mu,[†] Bin Zeng,[†] Peng Cheng,[†] Bing Shen,[†] and Hai-Hu Wen^{*,†,‡}

[†]National Laboratory for Superconductivity, Institute of Physics and Beijing National Laboratory for Condensed Matter Physics, Chinese Academy of Sciences, P.O. Box 603, Beijing 100190, China

[‡]National Laboratory of Solid State Microstructures and Department of Physics, Nanjing University, Nanjing 210093, China

ABSTRACT: We successfully synthesized the copper-based pnictide LiCu_2P_2 , which was reported as a superconductor with $T_c = 3.7$ K before. The temperature dependence of resistivity and DC magnetization was measured on both polycrystalline and single-crystalline LiCu_2P_2 . However, our repeatable synthesizing and measurements showed no superconducting transition either in resistivity or DC magnetization above 2 K. A metallic behavior can be seen in resistivity, and a Curie–Weiss behavior was observed in DC magnetization from 2 to 300 K. We have also carried out the Hall effect and MR measurements on the sample, from which we conclude that the LiCu_2P_2 has a single-band character. We also synthesized the polycrystalline $\text{Li}_{1-x}\text{Cu}_2\text{P}_2$, $\text{LiCu}_{2-x}\text{P}_2$, and $\text{Li}_{1+x}\text{Cu}_{2-x}\text{P}_2$ with different stoichiometries, and observed no superconductivity in all the samples.

The iron-based superconductors have formed a new family in the field of high- T_c superconductivity, since the discovery of superconductivity at 26 K in the layered quaternary compound $\text{LaFeAsO}_{1-x}\text{F}_x$.¹ Up to date, the family of the iron-based superconductors has been extended rapidly, including the so-called 1111 phase (LnFeAsO ,¹ AeFeAsF ,² Ln = rare earth elements, Ae = alkaline earth elements), 122 phase (AeFe_2As_2 , Ae = alkaline earth elements),³ 111 phase (LiFeAs , NaFeAs),⁴ and 11 phase (FeSe),⁵ 3442 phase ($\text{La}_3\text{Ni}_4\text{P}_4\text{O}_2$),⁶ and 21311 phase ($\text{Sr}_2\text{ScO}_3\text{-FeP}$, $\text{Sr}_2\text{VO}_3\text{FeAs}$).⁷ Very recently, the superconductivity in the copper-based pnictide LiCu_2P_2 was reported.⁸ The interesting point of this work is that the material LiCu_2P_2 has a basal plane similar to that of the iron pnictide superconductor; here in the Cu_2P_2 , however, the main player for possible superconductivity is Cu, not Fe. This would act as a bridge between the two types of high-temperature superconductors, namely the cuprates and the iron pnictides. However, in this work, our repeatable experiments gave a different result. There was not superconductivity observed in this compound.

By using a two-step solid-state reaction method, the polycrystalline samples of LiCu_2P_2 were fabricated. In the first step, Li foils and CuP powders, which were obtained by the prior chemical reactions from Cu and P powders, were mixed in the formula LiCu_2P_2 and pressed into a pellet shape. The pellet was placed in a Ta boat and sealed in a quartz tube with 0.2 bar of Ar gas, followed by a heat treatment at 170 °C for 20 h. In order to reduce the possible contamination of the samples with Ta, we did not wrap the sample with the Ta foil. After being cooled down slowly to room temperature, the pellet was ground adequately,

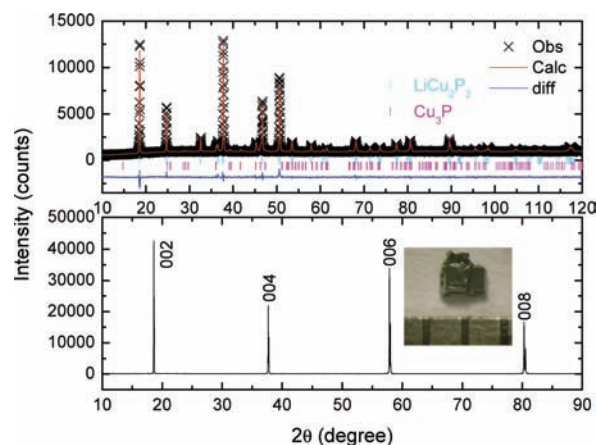


Figure 1. (Upper panel) X-ray powder diffraction patterns and Rietveld fit for the polycrystalline LiCu_2P_2 sample. (Lower panel) 00 l reflections from the basal plane of a cleaved LiCu_2P_2 single crystal. The inset shows a photograph of the single-crystal.

pressed into a pellet again, and annealed at 675 °C for 20 h. The single crystals of LiCu_2P_2 were grown in Sn flux. The starting materials in the ratio of Li:Cu:P:Sn = 1:2:2:15 were placed in an alumina crucible and sealed under vacuum in a quartz tube. The contents were then heated to 900 °C for 180 h. Subsequently the furnace was cooled down to 600 °C at a rate of 3.5 °C/h at which point the excess Sn was spun off with the aid of a centrifuge and cleaned off in an aqueous solution of hydrochloric acid. All the weighing, mixing, grinding, and pressing procedures were finished in a glovebox under argon atmosphere with the moisture and oxygen below 0.1 ppm.

The X-ray diffraction (XRD) measurement was carried out on the polycrystalline powders and plate-like single-crystal. The powder diffraction data was well fitted with the tetragonal LiCu_2P_2 phase with the space group of $I4/mmm$ and minor Cu_3P phase. Rietveld refinement of XRD patterns (Figure 1) gave a composition of the samples: 95% main phase LiCu_2P_2 and 5% minor impurity phase Cu_3P . The Rietveld refinement shown in the upper panel of Figure 1 gave good agreement between the data and the calculated profiles, and the agreement factors were as follows: $wR_p = 4.49\%$, $R_p = 3.33\%$. Lattice parameters for LiCu_2P_2 were determined to be $a = 3.89152(5)$ Å and $c = 9.56114(4)$ Å, which is close to the result reported previously.⁸ As shown in the lower panel of Figure 1, an X-ray diffraction scan of the basal plane reflections from a single crystal indicates that

Received: October 3, 2010

Published: January 25, 2011

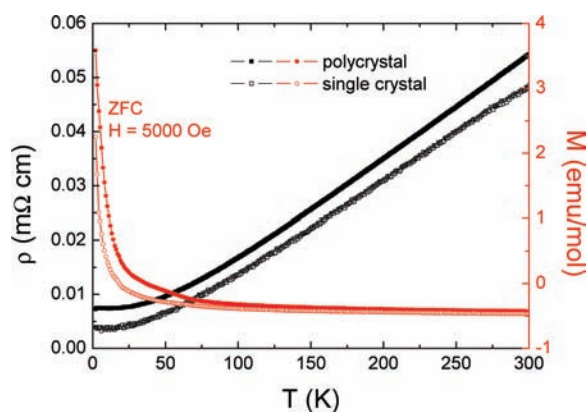


Figure 2. Temperature dependence of resistivity (black line) and dc magnetization for the zero-field cooling (ZFC) process at a magnetic field of $H = 5000$ Oe (red line) for the polycrystalline (solid symbols) and single-crystalline (open symbols) LiCu_2P_2 sample from 2 to 300 K.

the single crystal is chemically single phase. The peaks from the 00 l reflections are very sharp, indicating excellent crystalline quality. Using energy dispersive X-ray fluorescence spectroscopy (EDX), we did not find any trace of Sn impurities in our single-crystal samples.

The DC magnetization measurement was carried out on a Quantum Design superconducting quantum interference device (SQUID) magnetometer. The resistance data were collected using a four-probe technique on a Quantum Design instrument physical property measurement system (PPMS) with magnetic fields up to 9 T. In Figure 2 we present the temperature dependence of resistivity (black line) for both the polycrystalline and single-crystalline LiCu_2P_2 samples. A metallic behavior can be seen: The resistivity shows a linear relationship with the temperature above 50 K and levels off to a constant value (so-called residual resistivity) below 50 K. And the single-crystalline sample has a smaller residual resistivity. No superconductivity and resistivity anomaly corresponding to the SDW/structural transition⁹ were observed from 2 to 300 K. This can be further confirmed by the magnetization data (red line), which shows the temperature dependence of dc magnetization for the zero-field cooling process at 5000 Oe. A well-defined Curie–Weiss behavior was observed in the whole temperature region from 2 to 300 K, and no obvious magnetic transition was observed down to 2 K, which is different from iron-based parent compounds of FeAs-1111 phase¹² and FeAs-122 phase.¹⁰ This experiment has been repeated for several times with the same result.

To further understand the conducting carriers in the present sample, we also carried out the Hall effect measurements on the polycrystalline LiCu_2P_2 sample. The inset of Figure 3a shows the magnetic field dependence of Hall resistivity (ρ_{xy}) at different temperatures. In the experiment, ρ_{xy} was taken as $\rho_{xy} = [\rho(+H) - \rho(-H)]/2$ at each point to eliminate the effect of the misalignment of the Hall electrodes. It is clear that ρ_{xy} is positive at all temperatures below 300 K for LiCu_2P_2 leading to a positive Hall coefficient $R_H = \rho_{xy}/H$, which indicates that hole-type charge carriers dominate the conduction in the present sample. This is similar to that of the KFe_2As_2 parent phase but in sharp contrast to (Ca, Sr, Ba) Fe_2As_2 . However, hardly any temperature-dependent variation was observed in the whole temperature region, as shown in the mainframe of Figure 3a. One can see that R_H remains positive in wide temperature regime up to 300 K, and the absolute value of R_H remains as a constant within the error bars from 2 to 300 K, which possibly indicates a single-band character. The

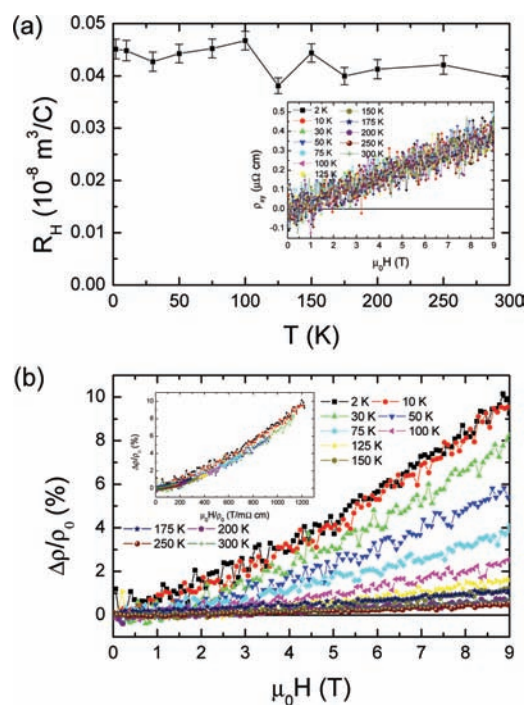


Figure 3. (a) Temperature dependence of Hall coefficient R_H determined on the polycrystalline LiCu_2P_2 sample. Positive values of R_H and very weak temperature dependence can be seen. Inset: The raw data of the Hall resistivity ρ_{xy} versus the magnetic field μ_0H at different temperatures. (b) Field dependence of MR for the present sample at different temperatures. The inset shows the Kohler plot of MR.

absolute value of R_H is remarkably small, indicating a relatively high density of charge carriers. Taking the average value of $R_H = 0.04287 \times 10^{-8} \text{ m}^3/\text{C}$ into the equation $R_H = 1/ne$, we can get the hole concentration $n = 1.4579 \times 10^{28}/\text{m}^3$.

The magnetoresistance (MR) is a very powerful tool to investigate the properties of electronic scattering.¹¹ Field dependence of MR for the polycrystalline LiCu_2P_2 sample at different temperatures is shown in the mainframe of Figure 3b. One can see a systematic evolution of the curvature in the $\Delta\rho/\rho_0$ vs H curve, where $\Delta\rho = \rho(H) - \rho_0$, $\rho(H)$ and ρ_0 represent the longitudinal resistivity at a magnetic field H and that at zero field, respectively. The data has an upward curvature, and the absolute value of $\Delta\rho/\rho_0$ decreases to zero with the increase of temperature. The semiclassical transport theory has predicted that the Kohler's rule will hold if only one isotropic relaxation time is present in a solid-state system.¹² The Kohler's rule can be written as $\Delta\rho/\rho_0 = F(H/\rho_0)$. This equation means that the $\Delta\rho/\rho_0$ vs H/ρ_0 curves for different temperatures, the so-called Kohler's plot, should be scaled to a universal curve if the Kohler's rule is obeyed. The scaling based on the Kohler plot of our sample is revealed in the inset of Figure 3b. It is clear that the curves at different temperatures can be scaled to a universal curve, which means that there is only one relaxation rate τ in the transport process in the temperature region of 2 to 300 K. It gives further support to the argument of single-band effect. If the superconductivity in iron pnictides is really induced by the interband scattering of electrons, this mechanism cannot apply to the LiCu_2P_2 , since a single-band feature dominates here.

To give convincing proof that other samples of LiCu_2P_2 may not be superconducting, we also synthesized the polycrystalline $\text{Li}_{1-x}\text{Cu}_2\text{P}_2$, $\text{LiCu}_{2-x}\text{P}_2$, and $\text{Li}_{1+x}\text{Cu}_{2-x}\text{P}_2$ with different

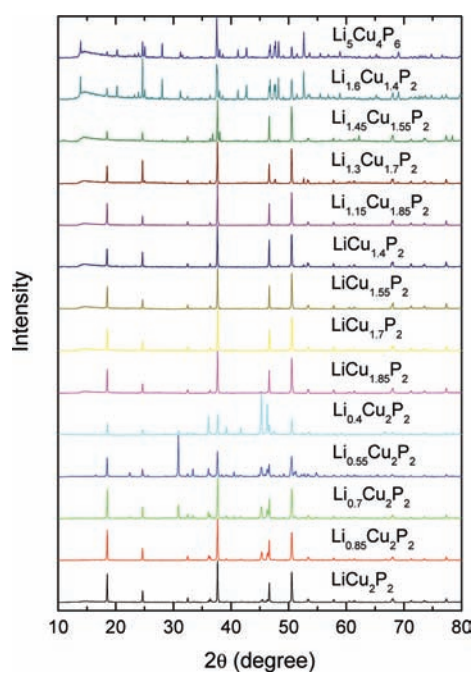


Figure 4. X-ray powder diffraction patterns for the polycrystalline $\text{Li}_{1-x}\text{Cu}_2\text{P}_2$, $\text{LiCu}_{2-x}\text{P}_2$, and $\text{Li}_{1+x}\text{Cu}_{2-x}\text{P}_2$ with different stoichiometries.

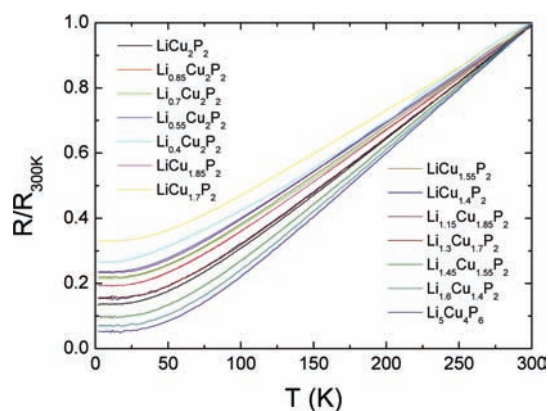


Figure 5. Temperature dependence of resistivity for the polycrystalline $\text{Li}_{1-x}\text{Cu}_2\text{P}_2$, $\text{LiCu}_{2-x}\text{P}_2$, and $\text{Li}_{1+x}\text{Cu}_{2-x}\text{P}_2$ with different stoichiometries.

stoichiometries, and measured the temperature dependence of resistivity. The X-ray powder diffraction patterns of all the samples shown in Figure 4 show a change in structure with varied stoichiometries. With the increase of the Li deficiency in the $\text{Li}_{1-x}\text{Cu}_2\text{P}_2$ system, the content of $\text{Li}_{1-x}\text{Cu}_2\text{P}_2$ decreases, the impurity phase Cu_3P or CuP_2 appears obviously, and the main peak of $\text{Li}_{1-x}\text{Cu}_2\text{P}_2$ shifts monotonically. This systematic evolution clearly indicates Li deficiency has been successfully induced. With the increase of the Cu deficiency in the $\text{LiCu}_{2-x}\text{P}_2$ system and the content of Li ions occupying the site of Cu ions in the $\text{Li}_{1+x}\text{Cu}_{2-x}\text{P}_2$ system, the main peaks of $\text{LiCu}_{2-x}\text{P}_2$ and $\text{Li}_{1+x}\text{Cu}_{2-x}\text{P}_2$ shift, too. When the Li ions substitute Cu ions to the stoichiometry as $\text{Li}_{1.67}\text{Cu}_{1.33}\text{P}_2$, the main phase changes to $\text{Li}_5\text{Cu}_4\text{P}_6$. We observe no superconductivity in the temperature dependence of resistivity for all the samples, as shown in Figure 5.

In summary, we successfully synthesized polycrystalline and single-crystalline LiCu_2P_2 samples and found no superconducting transition either in resistivity or DC magnetization above 2 K. We have also carried out the Hall effect and MR measurements on the polycrystalline sample, from which we conclude that the LiCu_2P_2 has a single-band character. And we found no superconductivity in the polycrystalline $\text{Li}_{1-x}\text{Cu}_2\text{P}_2$, $\text{LiCu}_{2-x}\text{P}_2$, and $\text{Li}_{1+x}\text{Cu}_{2-x}\text{P}_2$ with different stoichiometries.

AUTHOR INFORMATION

Corresponding Author

hhwen@aphy.iphy.ac.cn

ACKNOWLEDGMENT

This work is supported by the Natural Science Foundation of China, the Ministry of Science and Technology of China (973 Project: 2010CBA00100), the Knowledge Innovation Project of Chinese Academy of Sciences.

REFERENCES

- (1) Kamihara, Y.; Watanabe, T.; Hirano, M.; Hosono, H. *J. Am. Chem. Soc.* **2008**, *130*, 3296.
- (2) (a) Matsui, S.; Inoue, Y.; Nomura, T.; Yanagi, H.; Hirano, M.; Hosono, H. *J. Am. Chem. Soc.* **2008**, *130*, 14428. (b) Han, F.; Zhu, X.; Mu, G.; Cheng, P.; Wen, H.-H. *Phys. Rev. B* **2008**, *78*, 180503(R).
- (3) (a) Rotter, M.; Tegel, M.; Johrendt, D. *Phys. Rev. Lett.* **2008**, *101*, 107006. (b) Sasmal, K.; Lv, B.; Lorenz, B.; Guloy, A.-M.; Chen, F.; Xue, Y.-Y.; Chu, C.-W. *Phys. Rev. Lett.* **2008**, *101*, 107007.
- (4) (a) Wang, X.-C.; Liu, Q.-Q.; Lv, Y.-X.; Gao, W.-B.; Yang, L.-X.; Yu, R.-C.; Li, F.-Y.; Jin, C.-Q. *Solid State Commun.* **2008**, *148*, 538. (b) Tapp, J.-H.; Tang, Z.-J.; Lv, B.; Sasmal, K.; Lorenz, B.; Chu, P. C. W.; Guloy, A. M. *Phys. Rev. B* **2008**, *78*, 060505.
- (5) Hsu, F.-C.; Luo, J.-Y.; Yeh, K.-W.; Chen, T.-K.; Huang, T.-W.; Wu, P.-M.; Lee, Y.-C.; Huang, Y.-L.; Chu, Y.-Y.; Yan, D.-C.; Wu, M.-K. *Proc. Natl. Acad. Sci. U.S.A.* **2008**, *105*, 14262.
- (6) Klimczuk, T.; McQueen, T.-M.; Williams, A.-J.; Huang, Q.; Ronning, F.; Bauer, E.-D.; Thompson, J.-D.; Green, M.-A.; Cava, R.-J. *Phys. Rev. B* **2009**, *79*, 012505.
- (7) (a) Ogino, H.; Matsumura, Y.; Katsura, Y.; Ushiyama, K.; Horii, S.; Kishio, K.; Shimoyama, J. *Supercond. Sci. Technol.* **2009**, *22*, 075008. (b) Zhu, X.; Han, F.; Mu, G.; Cheng, P.; Shen, B.; Zeng, B.; Wen, H.-H. *Phys. Rev. B* **2009**, *79*, 220512(R).
- (8) Han, J.-T.; Zhou, J.-S.; Cheng, J.-G.; Goodenough, J. B. *J. Am. Chem. Soc.* **2010**, *132*, 908–909.
- (9) de la Cruz, C.; Huang, Q.; Lynn, J.-W.; Li, J.; Ratcliff, W., II; Zarestky, J.-L.; Mook, H.-A.; Chen, G.-F.; Luo, J.-L.; Wang, N.-L.; Dai, P. *Nature* **2008**, *453*, 899–902.
- (10) Rotter, M.; Tegel, M.; Schellenberg, I.; Hermes, W.; Pöttgen, R.; Johrendt, D. *Phys. Rev. B* **2008**, *78*, 020503(R).
- (11) (a) Li, Q.; Liu, B.-T.; Hu, Y.-F.; Chen, J.; Gao, H.; Shan, L.; Wen, H.-H.; Pogrebnjakov, A.-V.; Redwing, J.-M.; Xi, X. X. *Phys. Rev. Lett.* **2006**, *96*, 167003. (b) Yang, H.; Liu, Y.; Zhuang, C.-G.; Shi, J.-R.; Yao, Y.-G.; Massidda, S.; Monni, M.; Jia, Y.; Xi, X.-X.; Li, Q.; Liu, Z.-K.; Feng, Q.-R.; Wen, H.-H. *Phys. Rev. Lett.* **2008**, *101*, 067001.
- (12) Ziman, J.-M. *Electrons and Phonons*; Oxford Classic Texts in the Physical Sciences; Oxford University Press: New York, 2001.